jove

Quantitative 3D Imaging of *Trypanosoma cruzi*-Infected Cells, Dormant Amastigotes, and T Cells in Intact Clarified Organs

Fernando Sanchez-Valdez[1], **Ángel M. Padilla**[1], **Juan M. Bustamante**[1], **Caleb W. D. Hawkins**[1], **Rick L. Tarleton**[1,2]

[1] Center for Tropical and Emerging Global Diseases, University of Georgia [2] Department of Cellular Biology, University of Georgia

Corresponding Author

Fernando Sanchez-Valdez
nano2014@uga.edu

Citation

Sanchez-Valdez, F., Padilla, Á.M., Bustamante, J.M., Hawkins, C.W.D., Tarleton, R.L. Quantitative 3D Imaging of *Trypanosoma cruzi*-Infected Cells, Dormant Amastigotes, and T Cells in Intact Clarified Organs. *J. Vis. Exp.* (), e63919, doi:10.3791/63919 (2022).

Date Published

June 9, 2022

DOI

10.3791/63919

URL

jove.com/t/63919

Abstract

Chagas disease is a neglected pathology that affects millions of people worldwide, mainly in Latin America. The Chagas disease agent, *Trypanosoma cruzi* (*T. cruzi*), is an obligate intracellular parasite with a diverse biology that infects several mammalian species, including humans, causing cardiac and digestive pathologies. Reliable detection of *T. cruzi in vivo* infections has long been needed to understand Chagas disease's complex biology and accurately evaluate the outcome of treatment regimens. The current protocol demonstrates an integrated pipeline for automated quantification of *T. cruzi*-infected cells in 3D-reconstructed, cleared organs. Light-sheet fluorescent microscopy allows for accurately visualizing and quantifying of actively proliferating and dormant *T. cruzi* parasites and immune effector cells in whole organs or tissues. Also, the CUBIC-HistoVision pipeline to obtain uniform labeling of cleared organs with antibodies and nuclear stains was successfully adopted. Tissue clearing coupled with 3D immunostaining provides an unbiased approach to comprehensively evaluate drug treatment protocols, improve the understanding of the cellular organization of *T. cruzi*-infected tissues, and is expected to advance discoveries related to anti-*T. cruzi* immune responses, tissue damage, and repair in Chagas disease.

Introduction

Chagas disease, caused by the protozoan parasite *T. cruzi*, is among the world's most neglected tropical diseases, causing approximately 13,000 annual deaths. The infection often progresses from an acute to a chronic stage producing cardiac pathology in 30% of the patients, including arrhythmias, heart failure, and sudden death[1,2]. Despite the strong host immune response elicited against the parasite during the acute phase, low numbers of parasites chronically persist throughout the host's life in tissues such as the heart and skeletal muscle. Several factors, including the delayed onset of adaptive immune responses and the presence of non-replicating forms of the parasite, may contribute to

the capacity of *T. cruzi* to avoid a complete elimination by the immune system[3,4,5,6]. Furthermore, non-replicating dormant forms of the parasite display a low susceptibility to trypanocidal drugs and may in part be responsible for the treatment failure observed in many cases[7,8].

The development of new imaging techniques provides an opportunity to gain insight into the spatial distribution of the parasites in the infected tissues and their relationship with the immune cells involved in their control. These characteristics are crucial for a better understanding of the processes of parasite control by the immune system and tracking the rare dormant parasites present in chronic tissues.

Light-sheet fluorescence microscopy (LSFM) is one of the most comprehensive and unbiased methods for 3D imaging of large tissues or organs without thin-sectioning. Light-sheet microscopes utilize a thin sheet of light to only excite the fluorophores in the focal plane, reduce photobleaching and phototoxicity of samples, and record images of thousands of tissue layers using ultra-fast cameras. The high level of tissue transparency necessary for the proper penetration of the laser light in tissues is obtained by homogenizing the refractive index (RI) following tissue delipidation and decolorization, which reduces the scattering of light and renders high-quality images[9,10,11].

Tissue clearing approaches have been developed for the imaging of whole mice[12,13,14], organoids[15,16,17], organs expressing reporter fluorescent markers[18,19,20,21,22,23], and recently a limited number of human tissues[24]. The current methods for tissue clearing are classified into three families: (1) organic solvent-based methods such as DISCO protocols[25,26], (2) hydrogel-based methods, such as CLARITY[27], and aqueous methods, such as CUBIC (Clear, Unobstructed Brain/Body Imaging Cocktails and Computational analysis)[18,19,28,29]. CUBIC protocols maintain organ shape and tissue integrity, preserving the fluorescence of endogenously expressed reporter proteins. The most recent update of this technique, CUBIC-HistoVision (CUBIC-HV), also permits the detection of epitopes using fluorescently-tagged antibodies and DNA labeling[28].

In the present protocol, the CUBIC pipeline for detecting *T. cruzi* expressing fluorescent proteins in clarified intact mouse tissues was used. Optically transparent tissues were LSFM imaged, 3D reconstructed, and the precise total number of *T. cruzi* infected cells, dormant amastigotes, and T cells per organ were automatically quantified. Also, this protocol was successfully adopted to obtain uniform labeling of cleared organs with antibodies and nuclear stains. These approaches are essential for understanding the expansion and control of *T. cruzi* in infected hosts and are useful for fully evaluating chemo- and immuno-therapeutics for Chagas disease.

Protocol

This study was carried out in strict accordance with the Public Health Service Policy on Humane Care and Use of Laboratory Animals and Association for Assessment and Accreditation of Laboratory Animal Care accreditation guidelines. The Animal Use Protocol (control of *T. cruzi* infection in mice-A2021 04-011-Y1-A0) was approved by the University of Georgia Institutional Animal Care and Use Committee. B6.C+A2:A44g-Gt(ROSA)26Sor$^{tm14(CAG-tdTomato)Hze}$/J, B6.Cg-Gt(ROSA)26Sor$^{tm14(CAG-tdTomato)Hze}$/J and C57BL/6J-Tg(Cd8a*-cre)B8Asin/J mice (female, 1-2 months old) were used for the present study. The mice were obtained from commercial sources (see **Table of Materials**).

1. Infection, perfusion, and dissection

1. Intraperitoneally infect mice with tissue culture-derived trypomastigotes of Colombiana (DTU TcI) or Brazil (DTU TcV) *T. cruzi* strain expressing tdTomato or GFP fluorescent proteins, respectively. The infection dose could range from 50,000 to 200,000 trypomastigotes diluted in 100 µL of 1x Phosphate-Buffered Saline (PBS).
   NOTE: Specific details about the generation of reporter parasites and mouse models of infection are available in Canavaci et al.[29] and Bustamante et al.[30].
2. Euthanize the mice by carbon dioxide inhalation at a flow rate of 3-7 L/min. As soon as the animals stop showing any pedal reflex, make a longitudinal incision through the skin from the abdomen towards the sternum. Then cut the body wall from the abdomen and continue through the ribs on each side of the thorax until the sternum can be lifted away, exposing the heart.
3. As described in **Figure 1**, make a 2.5 mm incision in the heart's right auricle and collect the draining blood using a 1 mL micropipette tip.
4. Insert a butterfly needle (connected to one end of the perfusion system) into the apex of the left ventricle until it reaches the ascending aorta. Use gel-based glue (see **Table of Materials**) to seal the inlet hole around the needle and maintain the needle in position during perfusions.
5. Perfuse the mice[30] with 50 mL of cold Heparin-PBS (pH 7.4, 10 U/mL of Heparin) or until the fluid that comes out of the mouse toward the collection tray is clear of blood.
6. Perfuse with 50 mL of cold 4% (w/v) paraformaldehyde (PFA) (pH 7.4) in PBS.
   NOTE: PFA tissue fixation is likely one of the critical steps of the protocol, especially for maintaining epitope structures and subsequent immunodetection. PFA degrades over time, so it must be freshly prepared. The pH of the solution is also important to avoid over-fixation, which could lead to poor clearing of tissues.
   CAUTION: PFA is moderately toxic by skin contact. Acute exposure is also highly irritating to the nose, eyes, and throat. Long-term exposure to low levels in the air or skin may cause skin irritation such as dermatitis and itching, and asthma-like respiratory problems. Wear face and eye protection and do not breathe dust, gas, mist, fumes, or vapors.
   1. Following the PFA perfusion, perfuse the mouse with 100 mL of CUBIC-P buffer to reach the clarification levels mentioned in step 1.5.
   2. To prepare CUBIC-P buffer, dissolve 10% N-butyldiethanolamine, 5% Triton X-100, and 5% 1-N-Methylimidazole in double-distilled water or use the commercial cocktails (see **Table of Materials**).
      NOTE: Steps 1.6.1.-1.6.2. are recommended only for highly pigmented organs such as the heart and kidney since they require a pre-clearing step to obtain increased levels of transparency. After using CUBIC-P, dissect the organs and proceed directly to step 2: Tissue clearing.
7. Dissect the tissue samples/organs[30] to be imaged and post-fix them in 4% (w/v) PFA in PBS (~10 mL/whole organ) overnight (ON) at 4 °C with gentle shaking (no more than 5 x *g*) in 50 mL conical tubes.
   NOTE: All the incubations from hereafter must be performed on tubes laying horizontally at 20-30 °C protected from light.

8. Wash the sample in 10 mL of PBS (supplemented with 0.05% sodium azide (NaN_3) for 3 h (three times) at room temperature (RT) with gentle shaking (5 x *g*).

   NOTE: Tissues can be frozen by incubating in 10 mL of 30% sucrose in PBS with gentle shaking (5 x *g*) at 4 °C ON in 50 mL conical tubes. After tissues sink to the bottom of the tube, embed them in the OCT compound and keep them at -80 °C. Thaw at RT until the OCT compound completely melts, then wash in PBS (~10 mL/ whole organ) ON at 4 °C with gentle shaking (5 x *g*) in 50 mL conical tubes. Proceed to step 2.

2. Tissue clearing

NOTE: All the tissue clearings performed in this work were done using CUBIC protocol I[22]. Three different cocktails were used: CUBIC-P for delipidation and rapid decolorization during perfusions, CUBIC-L for delipidation and decolorization, and CUBIC-R for RI matching. DNA staining and immunostainings were performed using CUBIC-HV 1 3D nuclear staining kit and CUBIC-HV 1 3D immunostaining kit, respectively (see **Table of Materials**).

1. Immerse individual organs in 10 mL of 50% water-diluted CUBIC-L (see **Table of Materials**) with gentle shaking (5 x *g*) at RT (ON) in 50 mL conical tubes. Keep tubes flat on the shaking plate.

   NOTE: To avoid tissue damage, organs are maintained in the same tube, and solutions are collected using a vacuum system. To prepare CUBIC-L, dissolve 10% N-butyldiethanolamine and 10% Triton X-100 in double-distilled water using the commercial cocktails (see **Table of Materials**).

   CAUTION: CUBIC-L causes serious eye damage.Wear eye and face protection. Dispose to an approved waste disposal plant.

2. Immerse sample in 10 mL of 100% CUBIC-L for 6 days (refreshing the solution on day 3).

   NOTE: At the end of this incubation period, the tissues must be almost completely transparent.

3. Wash the transparent organs with PBS (supplemented with 0.05% NaN_3) for 2 h (three times) at 37 °C with gentle shaking (5 x *g*). Transfer tissues to a new 50 mL conical tube with each wash to remove Triton X-100.

   NOTE: As described in **Figure 2B**, if the goal of the experiment is to visualize endogenously-expressed reporter proteins from transgenic *T. cruzi* parasites or mice (**Figure 2C-F**), skip steps 3, 4, and 5 and continue directly to step 6.

3. DNA staining

1. Dilute the commercially available nucleic acid dye (see **Table of Materials**) in 5 mL of staining buffer (included in the kit) at 1/2,500 dilution.

2. Immerse tissue in the nuclear dye solution and incubate at 37 °C with gentle rotation for 5 days using 15 mL conical tubes in a standing position.

3. Wash with 15 mL of 3D nuclear staining wash buffer (included in the kit) for 2 h (three times) at RT with gentle shaking (5 x *g*).

   NOTE: Other DNA dyes can be used in these concentrations and incubation times: DAPI (included in the kit): 1/200, 5 days incubation; BOBO-1: 1/400, 5 days incubation; Propidium Iodide (PI) (included in the kit): 1/100, 3 days incubation; RedDot2: 1/250, 3 days incubation. If the specific aim of the experiment is to

visualize both endogenously-expressed reporter proteins and use nuclear stains, skip steps 4 and 5 and continue directly to step 6.

4. Extracellular matrix (ECM) digestion

NOTE: Hyaluronidase digestion of the ECM must be performed to facilitate the proper penetration of the antibodies into deep regions of the tissues[28].

1. Immerse individual organs in 15 mL of hyaluronidase reaction buffer for 2 h at 37 °C in a 50 mL conical tube in flat position protected from light.
   NOTE: To prepare hyaluronidase reaction buffer, dissolve 10 mM of CAPSO; 150 mM of Sodium Chloride (NaCl), and 0.05% of NaN_3 (see **Table of Materials**) in double-distilled water and adjust pH to 10.
2. Prepare Enzyme Solution by mixing 75 µL of 20 mg/mL of hyaluronidase stock into 425 µL of hyaluronidase reaction buffer. To prepare 20 mg/mL of hyaluronidase stock, dissolve hyaluronidase in 50 mM of Carbonate buffer, 150 mM of NaCl, 0.01% of BSA, and 0.05% of NaN_3 (see **Table of Materials**). Adjust pH to 10 and aliquot in volumes of 77 µL at -30 °C.
3. Discard hyaluronidase reaction buffer using a pipette and immerse the organ in the Enzyme Solution (500 µL in a 15 mL conical tube) in a standing position protected from light for 24 h at 37 °C with gentle shaking (5 x *g*).
4. Wash the sample in 15 mL of hyaluronidase wash buffer in a 50 mL conical tube in a horizontal position protected from light for 2 h (three times) at 37 °C with gentle shaking (5 x *g*).
   1. To prepare hyaluronidase wash buffer, dissolve 50 mM of Carbonate buffer, 150 mM of NaCl, 0.1% (v/v) of Triton X-100, 5% (v/v) of Methanol, and 0.05% NaN_3. Adjust pH to 10. To prepare 10x Carbonate buffer-NaCl stock, dissolve 2.96 g of Sodium Carbonate, 1.86 g of Sodium Hydrogen Carbonate, and 8.77 g of NaCl in 100 mL of double-distilled water with 0.05% NaN_3 (see **Table of Materials**) and adjust pH to 10.

5. Immunostaining

1. Label vasculature using anti-α-SMA (alpha-small muscle actin, see **Table of Materials**) antibodies following the steps below.
   1. Generate primary plus conjugated Fab fragment secondary antibody complex. Start this reaction 1.5 h prior to the staining procedure.
      1. Calculate the required amount of primary and secondary antibodies (mix at a 1:0.5 ratio by weight).
         NOTE: For the primary antibody anti-α-SMA, 3.5 µg is needed to label the entire heart or a fragment of skeletal muscle of similar dimensions. For 2.5 mg/mL product, 3.5/2.5 = 1.4 µL of antibody solution is needed. For secondary antibody AlexaFluor 647 anti-mouse Fab fragment, 1.75 µg is needed to label the entire heart or a fragment of skeletal muscle of similar dimensions. For 1.7 mg/mL product, 1.75/1.7 = 1 µL of antibody solution is needed.
      2. Mix primary and secondary antibodies in an amber 2 mL tube and incubate for 1.5 h at 37 °C.
   2. For buffer exchange, mix 7.5 mL of 2x HV1 3D immunostaining buffer (included in the kit, see **Table of Materials**) with 7.5 mL of double-distilled water and immerse the tissue sample for 1.5 h

at 32 °C with gentle shaking (5 x *g*) in a 15 mL conical tube in a horizontal position. Start this reaction simultaneously as the generation of antibody complex (1.5 h prior to the immunostaining procedure).

2. Perform 3D immunostaining following the steps below.
    1. In a 15 mL conical tube, prepare the antibody staining solution following **Supplementary File 1**.
    2. Collect the tissue sample from the buffer exchange media (step 5.1.2) and immerse it in the antibody staining solution. Incubate tissues individually for 1 week at 32 °C with gentle shaking (5 x *g*) of the tubes in a standing position protected from light. Seal the tube with paraffin film to avoid evaporation.
    3. Move to 4 °C and incubate ON in a standing position.
    4. Cool 1x HV1 3D immunostaining wash buffer (included in the kit, see **Table of Materials**) to 4 °C and wash the sample with 15 mL buffer (two times) for 30 min each at 4 °C with gentle shaking (5 x *g)*. Keep 15 mL conical tubes in a horizontal position until step 5.2.7.
    5. Dilute formalin to 1% in 1x HV1 3D immunostaining wash buffer and immerse the sample in 8 mL of the solution for 24 h at 4 °C with gentle shaking (5 x *g*).
    6. Incubate in fresh 1% formalin solution for 1 h at 37 °C with gentle shaking (5 x *g*).
    7. Wash in 15 mL of PBS for 2 h at 25 °C with gentle shaking (5 x *g*).
3. Boost tdTomato signal using anti-Red Fluorescent Protein (RFP) antibodies following the steps below.
    1. Follow the same incubation times and temperatures as in step 5.2.2. Calculate the amount of primary and secondary antibodies (see **Table of Materials**) and mix them at a 1:0.5 ratio by weight.

        NOTE: For primary antibody anti-RFP, 5 µg is needed to label the entire heart or a fragment of skeletal muscle of similar dimensions. For 1.25 mg/mL product, 5/1.25 = 4 µL of the solution is required. For secondary antibody Alexa Fluor 647 anti-rabbit Fab fragment, 2.5 µg is needed to label the entire heart or a fragment of skeletal muscle of similar dimensions. For 1.5 mg/mL product, 2.5/1.5 = 1.7 µL of the solution is needed.
    2. Prepare the antibody staining solution as mentioned in **Supplementary File 1**.
4. Boost GFP signals using anti-GFP nanobodies following the steps below.
    1. Follow the same incubation times and temperatures as mentioned in step 5.2.2.

        NOTE: Anti-GFP nanobodies (see **Table of Materials**) are conjugated with Alexa Fluor 647, so the antibody complex generation is unnecessary.
    2. Prepare the antibody staining solution as mentioned in **Supplementary File 1**.

6. RI matching

1. Immerse transparent organs in 5 mL of 50% water-diluted CUBIC-R+ solution (see **Table of Materials**) at RT (ON) with gentle shaking (5 x *g*) in a 50 mL conical tube. Keep tubes in a standing position during the entire RI matching step.

    NOTE: Recycled CUBIC R+ solutions from previous experiments could be reused (up to four times) in this step. To prepare CUBIC-R+ solution, dissolve 45% of 2,3-Dimethyl-1-phenyl-5-pyrazolone (Antipyrine), 30% of

Nicotinamide or N-Methylnicotinamide, and 0.5% of N-butyldiethanolamine in double-distilled water or use the commercial CUBIC-R+ buffer (see **Table of Materials**).

CAUTION: CUBIC-R+ causes skin irritation, serious eye irritation, and damage to organs. Wear protective gloves, and ensure eye and face protection. Do not breathe dust, fumes, gas, mist, or vapors. Dispose of to an approved waste disposal plant.

2. Replace 50% CUBIC-R+ with 5 mL of 100% CUBIC-R + and incubate with gentle shaking (5 x *g*) at RT for 2 days. Then, transfer the tissues onto a stack of lint-free wipes and carefully turn the tissues to remove CUBIC-R + solution from the organ surfaces for 5 min.

7. Mounting

1. After drying the tissues, transfer them to 5 mL of Mounting Solution (RI = 1.520) (see **Table of Materials**) in a six-well cell culture plate and incubate them (ON) at RT. Frequently turn the tissues to eliminate air bubbles, especially on the surfaces of the organs.

   NOTE: Organs can be stored for more than 6 months in Mounting Solution or CUBIC-R+.

2. Adhere the tissues to the microscope sample holder by using cyanoacrylate-based gel glue.

3. Immerse the samples in the microscope quartz cuvette filled with 120 mL of Mounting Solution and image them transversally to their longitudinal axis. Adhere the heart with the apex and the aorta horizontally aligned.

   NOTE: Cleared and mounted organs can be sectioned with a vibratome and imaged at high magnification by confocal microscopy. Embed the organs in 2% agarose and cut sections of 100-500 µm. Organs can also be manually sectioned with a sharp blade to produce thick-tissue sections (>1000 µm). After sectioning, place the slices into glass-bottom 35 mm Petri dishes, mount using the same mounting solution, seal with nail polish, and image with a confocal microscope.

8. Image acquisition

1. Image the mounted samples with a light-sheet microscope (see **Table of Materials**). Set magnification and step size between individual slices to 3 µm, and use right and left light sheet lasers with 5 µm thicknesses and 100% width. Set the exposure time constant at 50-100 ms, and adjust the laser power from 10% to 80% depending on the fluorescence signal intensity.

   1. For the co-detection of tdTomato-expressing parasites and DiR-stained dormant amastigotes (**Figure 2C**), use red (Ex/Em 561/620-660 nm) and infra-red (Ex/Em 785/845-55 nm) channels, respectively. For the co-detection of T cells and tdTomato-expressing parasites in CD8 reporter mouse (**Figure 2D**), use green (Ex/Em 488/525-50 nm) and red channel, respectively.

   2. For the coinfections assays (**Figure 2E**), as well as for the co-detection of parasites expressing GFP in nuclei reporter mice (**Figure 2F**), use the green and red channels, respectively. For the detection of tdTomato-expressing parasites, nuclear dye, and heart vasculature (**Figure 3B,C**), use the red, green, and far-red (Ex/Em 640/680-730 nm) channels, respectively.

   3. Detect anti-RFP antibodies with the far-red channel and anti-GFP nanobodies using the green channel (**Figure 3D**).

2. Convert the acquired TIFF image stacks and 3D reconstruct the organs using Imaris v9.7.2 software (see **Table of Materials**).

9. Surface reconstruction and quantification with Imaris software

1. Select **surfaces detection algorithm** tool and initiate the wizard in the image analysis software.
2. Perform an initial analysis in a 3D region of interest (randomly selected) and then apply it to the entire 3D organ reconstruction. After choosing a **region of interest (ROI)**, select the **channel** to be analyzed, uncheck the **smooth button**, and select **background subtraction**.
   NOTE: Background subtraction calculates a unique local background value for every voxel and subtracts this from the original pixel value. The diameter of the largest sphere which fits into the object must be up to 200 µm for *T. cruzi*-infected cells, 10 µm for T cells, and 5 µm for individual parasites.
3. Use the **histogram** to adjust the classification and the filter drop-down list to select the **measurements for classification**.
   NOTE: Use the histogram to adjust the classification: ellipticity (oblate) and sphericity measurements are recommended.
4. Finalize the wizard, press **statistics** button, and retrieve the total number of parasite-infected cells or T cells as the number of disconnected components per time point.

Representative Results

CUBIC fixed tissues were washed with PBS to remove fixatives and then incubated with CUBIC-L cocktails, a basic buffered solution of amino alcohols that extract pigments and lipids from the tissue resulting in decolorization of tissue while maintaining tissue architecture. Grid lines in the paper can be seen through the tissues indicating an appropriate clearing of the organs **(Figure 2A)**. After delipidation, tissues were washed and immersed in CUBIC-R+ and mounting solution for RI homogenization and imaging, respectively **(Figure 2B)**.

A wild-type mouse was infected with tdTomato-expressing trypomastigotes pre-stained with the DiR near-infrared cyanine dye. The mouse was euthanized 15 days post-infection, and the intact heart was dissected, fixed, and cleared. LSFM imaging and 3D reconstruction allowed us to visualize tdTomato-expressing proliferating *T. cruzi* parasites (red). Autofluorescence levels in the red channel can be used for the correct visualization of heart structure and edges **(Figure 2C i)**. LSFM was also useful for identifying drug-resistant dormant forms[7,8]. Pre-infection staining of parasites with DiR dye allows for the tracking of dormant parasites by visualizing the parasites that had not diluted the dye through replication, as previously reported for CellTrace Violet[7].

Dormant parasites (cyan) can be identified in the heart as depicted in the 3D enlarged insets (yellow arrows) **(Figure 2C ii,iii)**. Z-projection fluorescence was segmented automatically to generate a reconstructed 3D surface model for spatial visualization and quantification of the total number of *T. cruzi*-infected cells and dormant parasites throughout the entire 3D reconstruction **(Figure 2A).** Analysis of the 3D surface model revealed 186 *T. cruzi*-infected cells with a higher proportion of infected cells in the heart atrium (123) compared with ventricles (63) and 18 dormant parasites in the whole heart **(Figure 2C i)**. In a previous report, a similar pipeline to monitor the number of *T. cruzi*-infected cells and dormant parasites in clarified mice tissues after drug treatment was reported[31]. It is important to note that the estimates for numbers of dormant parasites are likely an undercount, as the dye dilution

technique allows detection only of parasites that have not replicated significantly since the initial infection, but does not detect those that became dormant later in the infection following multiple rounds of division.

A similar approach was used to monitor the interaction between different *T. cruzi* strains in interferon (IFN)-gamma deficient mice. The production of IFN-gamma by effector T cells is essential for the immune control of *T. cruzi*. In IFN-gamma knock-out mice, parasites proliferate with minimal immune restriction, yielding very high numbers of infected cells in organs. These immunodeficient models are useful tools for studying the efficacy of new drugs without the restriction imposed by immune recognition, and thus allow the detection of parasite relapse after treatment.IFN-gamma deficient mice were coinfected with tdTomato-expressing Colombiana (red) and GFP-expressing Brazil (blue) *T. cruzi* strains. The mice were euthanized 17 days post-infection, and the intact hearts were dissected, fixed, and cleared. In this immunodeficient model, host cells infected with both *T. cruzi* strains can be observed at various stages of parasite development, including large, medium, and small infected cells and recently burst ones. Slicing through the tissues shows abundant parasite-infected cells in the heart atria at various tissue depths **(Figure 2E i-iii** and **Movie 1)**.

A cross of C57BL/6J-Tg(Cd8a*-cre)B8Asin/J and B6.Cg-Gt(ROSA)26Sor $^{tm14(CAG-tdTomato)Hze}$/J mice, in which all T cells express the green fluorescent protein ZsGreen1, were used to monitor T cell recruitment in *T. cruzi* infected tissues. Mice were euthanized 14 days after infection with tdTomato-expressing parasites, and skeletal muscle was excised, cleared, and imaged by LSFM. ZsGreen1 expressing T cells (blue); additionally, *T. cruzi*-infected cells (red) were robustly detected **(Figure 2D i** and **Movie 2).** 3D zoom-ins of the 3D reconstruction identified T cells in the region of an infected cell **(Figure 2D ii).** Vibratome thick sections (200-500 µm) of the same tissue allow us to visualize the interface of T cells and host infected cells by confocal microscopy **(Figure 2D iii).**

An alternative way to monitor inflammation foci is based on cell nuclei accumulation around *T. cruzi*-infected cells. A reporter mouse wherein all cell nuclei express the fluorescent tdTomato protein was used for this purpose. The nuclear tdTomato expression (red) was easily detected in the tissues after the clearing process. A nuclear reporter mouse was infected with GFP-expressing *T. cruzi* parasites (cyan), and 35 days post-infection, was euthanized, and skeletal muscles were excised, cleared, and imaged by LSFM **(Figure 2F i-iii).** Zoomed optical sections of skeletal muscle reveal increased cellularity by accumulating red nuclei along GFP-expressing parasites **(Figure 2F ii)**. Vibratome sections of the same tissue confirm the previously described accumulation of red nuclei along GFP-expressing parasites by confocal microscopy **(Figure 2F iii)**.

CUBIC protocol was also adapted for immunostaining and DNA labeling of intact, cleared organs and tissues infected with *T. cruzi* **(Figure 3A)**. Mice were euthanized 40 days after infection with tdTomato-expressing parasites, and the hearts were dissected, fixed, and cleared. The intact cleared heart was washed and stained for 5 days with a green DNA marker, then washed again and immunostained for 7 days with antibodies against α-SMA. The samples were post-fixed, washed, RI matched, and imaged with LSFM. Simultaneous detection of multiple fluorescent signals, including nuclei, vasculature, and *T. cruzi*-infected cells, was possible following this protocol. α-SMA immunostaining (white) presented high signal levels revealing the intricate vasculature of the heart **(Figure 3B ii** and **Movie 3).**

An optical section from deeper heart regions depicts the tissue penetration of α-SMA antibodies in the established conditions **(Figure 3B v).** DNA staining (blue) also exhibited good tissue penetration, fluorescence levels, and stable volumetric staining. Some areas with intense DNA labeling were identified in different heart locations **(Figure 3B i)** and around skeletal muscle fibers **(Figure 3C i** and **Movie 4)**. A zoomed image of skeletal muscle showed an accumulation of blue nuclei in areas with few or undetectable tdTomato parasites, suggesting the recruitment of immune cells at sites of current or prior *T. cruzi* infection **(Figure 3C ii)**. In other cases, infected host cells had little to no evidence of nearby cellular infiltrates (white arrows) (**Figure 3C** i). Vibratome sections of the same tissue as in **Figure 3C** ii show DNA staining of cells and tdTomato-expressing parasites by confocal microscopy **(Figure 3C iii).**

Previous experiments have shown that dormant parasites exhibited low or negligible expression of tdTomato or GFP reporter proteins **(Figure 2C ii** and **iii)**. To improve the detection of these fluorescent proteins, cleared tissues were immunostained with anti-RFP or -GFP antibodies. Intact skeletal muscle tissues from mice infected with parasites expressing tdTomato or GFP were fixed, clarified, and immunostained with antibodies against RFP (RFP Booster) **(Figure 3D)** or nanobodies against GFP conjugated with Alexa Fluor 647 (GFP Booster) **(Figure 3E)**, respectively. The samples were post-fixed, washed, RI matched, and imaged with LSFM. In both cases, the boosting of the GFP and tdTomato signals by the antibodies resulted in strong fluorescence **(Figure 3D ii** and **3E ii)**. The immunostainings using boosting antibodies represent a versatile tool that will be used to detect *T. cruzi* dormants in clarified whole organ and tissues and detect any underrepresented signal from RFP or GFP family member's reporter proteins.

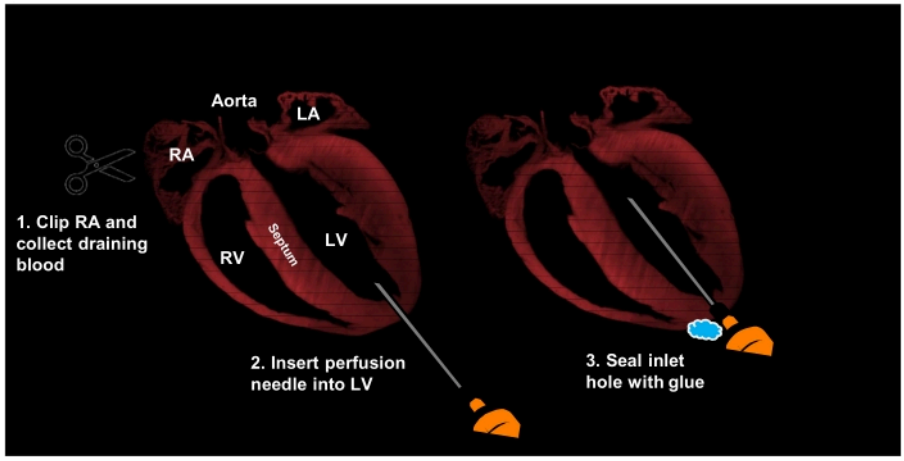

Figure 1: Needle insertion during transcardiac perfusion. (A) A schematic representation showing the steps performed before perfusing the mouse through the heart and the correct position and direction of the perfusion needle in the left ventricle. A small incision in the right atrium was performed, and draining blood was collected (1); a butterfly needle was inserted into the heart apex. Maintain the direction so that the needle does not pierce through the septum (2). The inlet

hole around the needle was sealed using gel-based glue (3). The liver is filled with blood and appears red before perfusion; however, after perfusion, it loses pigmentation and becomes pale. RA, right auricle; LA, left auricle; RV, right ventricle; LV, left ventricle. Please click here to view a larger version of this figure.

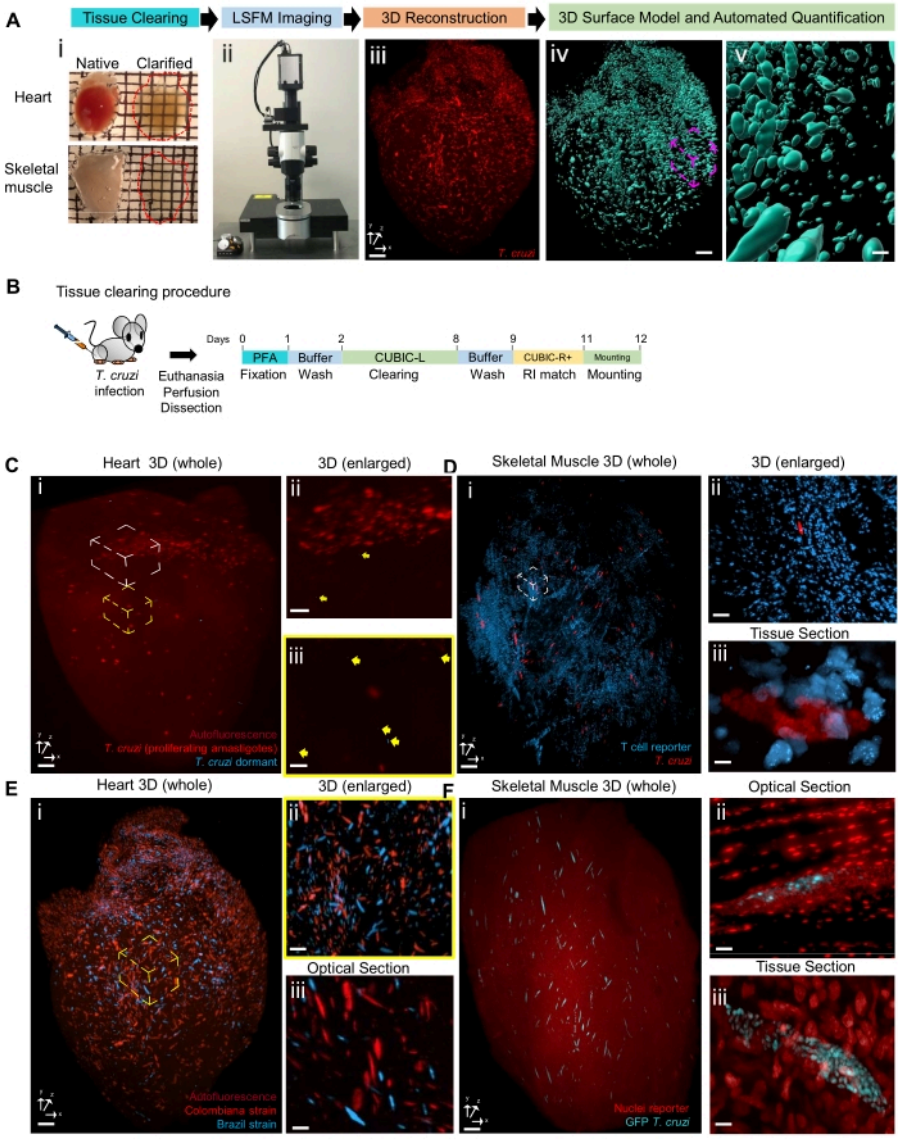

Figure 2: Visualization of *T. cruzi*-infected cells, dormant amastigotes, and inflammation foci in cleared organs. **(A)** Scheme of whole-organ *T. cruzi*-infected cells detection using tissue clearing, LSFM imaging, and software-assisted quantification in 3D surface models. (**i**) Bright-field images of the heart and skeletal muscle before (left) and after (right) clearing (scale bar: 1000 µm). (**ii**) Light-sheet fluorescence microscope. (**iii**) IFN gamma-deficient mouse was infected with 2 x 10^5 tdTomato-expressing trypomastigotes. At 17 days post-infection, the heart was dissected, CUBIC cleared, and LSFM imaged (scale bar: 500 µm). (**iv**) Z-projection fluorescence was segmented automatically to generate a reconstructed 3D surface model for spatial visualization and quantification of the number of *T. cruzi*-infected cells. A total of 736 *T. cruzi*-infected cells were detected in the whole heart (scale bar: 500 µm). (**v**) shows magnifications of the indicated volume in (**iv**), where cyanobjects represent *T. cruzi*-infected cells (scale bar: 50 µm). (**B**) Protocol of CUBIC whole-organ clearing. (**C**)

Visualization of proliferating and dormant *T. cruzi* parasites in transparent mouse heart. (**i**) A wild-type mouse was infected with 2 x 10^5 tdTomato-expressing trypomastigotes stained with a DiR near-infrared cyanine dye. The heart was dissected, cleared, and LSFM imaged. tdTomato-expressing proliferating (red) and dormant (cyan) *T. cruzi* parasites can be identified. Autofluorescence levels were maintained to allow for correct visualization of the heart structure. A mouse was killed 15 days post-infection based on the peak of parasite-infected cells and dormant amastigotes found in previous works (scale bar: 400 µm). (**ii**) and **(iii)** show magnifications of the indicated volume in (**i**), where yellow arrows indicate dormant parasites (cyan) (scale bar: 200 µm). (**D**) Detection of T cell recruitment in infected CD8 reporter mouse. (**i**) Reporter mouse was infected with 2 x 10^5 tdTomato-expressing trypomastigotes, and skeletal muscle was dissected, cleared, and LSFM imaged 14 days post-infection, a time point at which substantial cell responses are detected. ZsGreen1 expressing T cells (blue) as well as *T. cruzi*-infected cells (red) were visualized (scale bar: 400 µm) (see also **Movie 2**). (**ii**) shows magnifications of the indicated volume in (**i**) (scale bar: 50 µm). (**iii**) depicts T cell accumulation surrounding a *T. cruzi*-infected cell in a tissue section (200 µm) of the same organ (scale bar: 8 µm). (**E**) Interaction between different *T. cruzi* strains. (**i**) IFN-gamma deficient mice were coinfected with 2 x 10^5 tdTomato-expressing Colombiana (red) and GFP-expressing Brazil (blue) *T. cruzi* strains. The mice were euthanized, and the intact hearts were dissected, fixed, and cleared at 17 days post-infection (scale bar: 400 µm). (**ii**) shows magnifications of the indicated volume in (**i**) (scale bar: 250 µm). (**iii**) shows a magnified optical section revealing cells infected with Colombiana (red) and Brazil (blue) *T. cruzi* strains (scale bar: 150 µm). (**F**) Visualization of cellularity along infected cells using nuclei reporter mouse. (**i**) A nuclear reporter mouse was infected with 2 x 10^5 GFP-expressing trypomastigotes, and skeletal muscle was dissected, cleared, and LSFM imaged at 35 days post-infection. Nuclear tdTomato expression of the host cells (red), as well as GFP parasite expression (cyan), were detected (scale bar: 400 µm). (**ii**) shows a magnified optical section revealing accumulation of red nuclei along GFP-expressing parasites (scale bar: 90 µm). (**iii**) confirms increased cellularity by confocal imaging of tissue sections from the same organ (scale bar: 8 µm). Please click here to view a larger version of this figure.

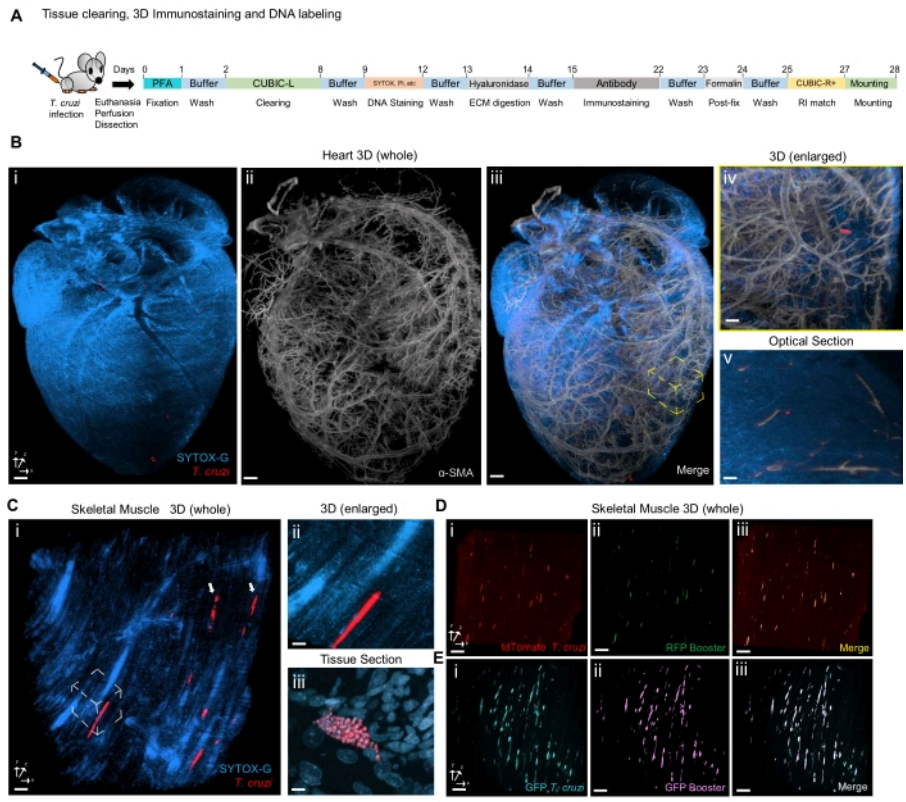

Figure 3: Labeling of cleared *T. cruzi*-infected organs with antibodies and nuclearstains. (**A**) CUBIC protocol for tissue clearing, 3D immunostaining, and DNA labeling of entire organs. (**B**) Labeling of mouse heart for vasculature and DNA detection (see also **Movie 3**). (**i-iii**) A wild-type mouse was infected with 2 x 10^5 tdTomato-expressing parasites. The mouse was euthanized 40 days after infection, and the heart was dissected, fixed, and cleared. The cleared heart was labeled with a DNA marker and immunostained with antibodies against α-SMA. Simultaneous detection of cell nuclei (blue), vasculature (white), and *T. cruzi*-infected cells (red) were possible. The mouse was killed at this time post-infection when tissue and special vasculature remodeling can be assessed (scale bar: 400 µm). (**iv**) shows a magnified volume from deep heart regions of (**iii**) depicting cell nuclei, vasculature, and infected cells (scale bar: 90 µm). (**v**) depicts an optical section obtained of (**iii**) (scale bar: 90 µm). (**C**) Increased cellularity visualized by DNA labeling of whole cleared skeletal muscle. (**i**) Skeletal muscle tissue from the previous experiment was DNA stained, revealing areas with intense nuclear labeling (blue) as well as *T. cruzi*-infected cells (red) (scale bar: 200 µm) (see also **Movie 4**). (**ii**) reveals an intense accumulation of blue nuclei in areas with lower to no detection of tdTomato parasite (scale bar: 100 µm). (**iii**) high magnification (60x) confocal imaging identifies DNA labeling of cells and parasites in tissue sections (scale bar: 10 µm). (**D**) Boosting of tdTomato parasite reporter markers in whole cleared skeletal muscle. (**i-iii**) Intact skeletal muscle tissues from mice infected with 2 x 10^5 parasites expressing tdTomato were fixed, clarified, and immunostained with antibodies against RFP (RFP Booster). An intense and uniform fluorescent signal was obtained in the far-red channel after RFP boosting (green) of the tdTomato signal

(red) (scale bar: 100 µm). (**E**) Boosting of GFP parasite reporter markers using anti-GFP nanobodies. (**i-iii**) Skeletal muscle tissues from mice infected with 2 x 10^5 parasites expressing GFP were fixed, clarified, and immunostained with Alexa Fluor 647-conjugated nanobodies against GFP (GFP Booster). A strong fluorescent signal was obtained in the far-red channel after GFP boosting (magenta) of the GFP fluorescence (cyan). Mouse from (**D**) and (**E**) were killed 30 days post-infection because parasite loads reach a peak at this time point, and parasite-infected cells can be easily detected in skeletal muscle (scale bar: 100 µm). Please click here to view a larger version of this figure.

Movie 1: *T. cruzi* infection of the heart and skeletal muscle in IFN-gamma deficient mice. 3D reconstructions of CUBIC-clarified tissues of IFN-gamma deficient mice coinfected with 2 x 10^5 tdTomato-expressing Colombiana (red) and GFP-expressing Brazil (blue) *T. cruzi* strains at day 17 post-infection. A total of 1151 individual slices of the heart and 559 of the skeletal muscle were acquired *via* LSFM. Comparable imaging results were achieved in three independent animals. Please click here to download this Movie.

Movie 2: Detection of T cell recruitment in *T. cruzi*-infected CD8 reporter mouse. 3D visualization of a CUBIC-clarified skeletal muscle from a CD8 reporter mouse infected with 2 x 10^5 Tdtomato-expressing Colombiana *T. cruzi* strain (red) and killed at 14 days post-infection. A total of 668 individual slices of the skeletal muscle were imaged by LSFM. ZsGreen1 expressing T cells (blue) as well as *T. cruzi*-infected cells (red) were visualized. Comparable imaging results were achieved in two animals. Please click here to download this Movie.

Movie 3: Immunodetection of vasculature in *T. cruzi*-infected and cleared heart. 3D reconstruction of a CUBIC-clarified heart of wild-type mice infected with 2 x 10^5 tdTomato-expressing Colombiana *T. cruzi* and immunostained with antibodies against α-SMA (blue) at 40 days post-infection. Slicing through the heart reveals the intricate vasculature of the heart and the tissue penetration of the α-SMA antibodies. Parasite infected cells could be observed as bright red spots in the heart atria (red, right). Comparable imaging results were achieved in two animals. Please click here to download this Movie.

Movie 4: Whole-organDNA staining reveals areas with increased cellularity. 3D reconstruction of the CUBIC-clarified skeletal muscle of wild-type mouse at 40 days post-infection infected with 2 x 10^5 tdTomato-expressing Colombiana *T. cruzi* strain. The whole quadriceps muscle area was stained with a green nuclear dye. *T. cruzi*-infected cells (red) and the nuclei of every cell in the tissue (blue) were visualized. Zoom-ins of the 3D reconstruction reveals accumulation of blue nuclei along areas with few or no detection of tdTomato parasites. Comparable imaging results were achieved in two animals. Please click here to download this Movie.

Supplementary File 1: Composition of the antibody staining solutions used in the study. Please click here to download this File.

Discussion

The absence of extensive, whole-organ imaging of parasites and the immune response limits the understanding of the complexity of the host-parasite interactions and impedes the evaluation of therapies for Chagas disease. The present study adopted the CUBIC pipeline to clarify and stain intact organs and tissues of *T. cruzi*-infected mice.

Multiple tissue clearing protocols were tested in this study (PACT[32], ECi[33], FLASH[34], iDISCO[11,26], and fDISCO[13]); however, only CUBIC preserved high levels of tdTomato or GFP parasite fluorescence. Similarly, previous reports showed the CUBIC preservation of endogenously expressed markers compared with other tissue-clearing approaches[35].

Limited resolution capacity is one of the current caveats of conventional light-sheet microscopy. This is clear in the difficulties of resolving individual parasites in heavily infected cells (**Figure 2C**). The newly developed tiling light-sheet microscopes with an improved resolution capacity and the adaptation of tissue expansion techniques could solve this problem[36].

Impurities from the washing buffers, clearing solutions, or other organs may precipitate in the tissue, producing nonspecific signals that may be mistaken for parasite-infected cells, individual parasites, or other structures. However, these artifacts usually fluoresce brightly in multiple channels, so after image analysis, they can be easily discarded from automated counting by imaging tissues in an alternative channel (usually the green channel). Double color objects were considered artifacts and excluded for automated quantification.

Nuclear stains DAPI, PI, RedDot2, and SYTOX-G, present good levels of tissue penetration and signal intensities in most of the CUBIC-cleared organs; however, the green DNA dye showed the best performance **(Figure 3B,C** and **Movie 4)**.

These results showed that *T. cruzi*-infected cells could be easily detected and accurately quantified while simultaneously identifying T cell or nuclei reporter mice signals. Most importantly, LSFM detected rare biological events, such as DiR-positive dormant amastigotes, within a complex tissue environment with the potential ability to expand it to epitope immunostaining and DNA labeling. Current studies are also exploring the utility of these approaches for monitoring the activation of immune effector cells, the interactions between multiple parasite strains in the same host, and the induction of tissue damage and repair in Chagas disease.

Disclosures

The authors declare that they have no competing interests.

Acknowledgments

We thank Dr. Etsuo Susaki for their valuable help and recommendations regarding tissue-clearing and immunostaining protocols. Also, we are grateful to M. Kandasamy from the CTEGD Biomedical Microscopy Core for technical support using LSFM and confocal imaging. We also thank all the members of Tarleton Research Group for helpful suggestions throughout this study.

References

1. Schofield, C. J., Jannin, J., Salvatella, R. The future of Chagas disease control. *Trends in Parasitology.* **22** (12), 583-588 (2006).
2. Marin-Neto, J. A., Cunha-Neto, E., Maciel, B. C., Simoes, M. V. Pathogenesis of chronic Chagas heart disease. *Circulation.* **115** (9), 1109-1123 (2007).
3. Tarleton, R. L. CD8+ T cells in Trypanosoma cruzi infection. *Seminars in Immunopathology.* **37** (3), 233-238 (2015).
4. Padilla, A. M., Simpson, L. J., Tarleton, R.L. Insufficient TLR activation contributes to the slow development of

CD8+ T cell responses in Trypanosoma cruzi infection. *Journal of Immunology.* **183** (2), 1245-1252 (2009).

5. Basso, B. Modulation of immune response in experimental Chagas disease. *World Journal of Experimental Medicine.* **3** (1), 1-10 (2013).
6. Martin, D. L. et al. CD8+ T-Cell responses to Trypanosoma cruzi are highly focused on strain-variant trans-sialidase epitopes. *PLOS Pathogens.* **2** (8), e77 (2006).
7. Sanchez-Valdez, F. J., Padilla, A., Wang, W., Orr, D., Tarleton, R. L. Spontaneous dormancy protects Trypanosoma cruzi during extended drug exposure. *Elife.* **7**, e34039 (2018).
8. Sanchez-Valdez, F., Padilla, A. In situ detection of dormant Trypanosoma cruzi amastigotes using bioluminescent-fluorescent reporters. *Methods in Molecular Biology.* **1955**, 179-186 (2019).
9. Vieites-Prado, A., Renier, N. Tissue clearing and 3D imaging in developmental biology. *Development.* **148** (18), 199369 (2021).
10. Ueda, H. R. et al. Tissue clearing and its applications in neuroscience. *Nature Reviews Neuroscience.* **21**, 61-79 (2020).
11. Molbay, M., Kolabas, Z. I., Todorov, M. I., Ohn, T. L., Erturk, A. A guidebook for DISCO tissue clearing. *Molecular Systems Biology.* **17**, e9807 (2021).
12. Pan, C. et al. Deep learning reveals cancer metastasis and therapeutic antibody targeting in the entire body. *Cell.* **179** (7), 1661-1676 (2019).
13. Qi, Y. et al. FDISCO: Advanced solvent-based clearing method for imaging whole organs. *Science Advances.* **5**, eaau8355, (2019).
14. Cai, R. et al. Panoptic imaging of transparent mice reveals whole-body neuronal projections and skull-meninges connections. *Nature Neuroscience.* **22**, 317-327 (2019).
15. Dekkers, J.F. et al. High-resolution 3D imaging of fixed and cleared organoids. *Nature Protocols.* **14**, 1756-1771 (2019).
16. Sachs, N. et al. Long-term expanding human airway organoids for disease modeling. *The EMBO Journal.* **38** (4), e100300 (2019).
17. Hu, H. et al. Long-Term Expansion of Functional Mouse and Human Hepatocytes as 3D Organoids. *Cell.* **175** (6), 1591-1606 (2018).
18. Susaki, E. A. et al. Whole-brain imaging with single-cell resolution using chemical cocktails and computational analysis. *Cell.* **157** (3), 726-739 (2014).
19. Susaki, E. A. et al. Advanced CUBIC protocols for whole-brain and whole-body clearing and imaging. *Nature Protocols.* **10**, 1709-1727 (2015).
20. Chung, K. et al. Structural and molecular interrogation of intact biological systems. *Nature.* **497**, 332-337 (2013).
21. Tainaka, K. et al. Whole-body imaging with single-cell resolution by tissue decolorization. *Cell.* **159** (4), 911-924 (2014).
22. Tainaka, K. et al. Chemical landscape for tissue clearing based on hydrophilic reagents. *Cell Reports.* **24** (8), 2196-2210 (2018).
23. Murakami, T. C. et al. A three-dimensional single-cell-resolution whole-brain atlas using CUBIC-X expansion microscopy and tissue clearing. *Nature Neuroscience.* **21**, 625-637 (2018).

24. Zhao, S. et al. Cellular and molecular probing of intact human organs. *Cell.* **180** (4), 796-812 (2020).

25. Erturk, A. et al. Three-dimensional imaging of solvent-cleared organs using 3DISCO. *Nature Protocols.* **7**, 1983-1995 (2012).

26. Renier, N. et al. iDISCO: a simple, rapid method to immunolabel large tissue samples for volume imaging. *Cell.* **159** (4), 896-910 (2014).

27. Chung, K., Deisseroth, K. CLARITY for mapping the nervous system. *Nature Methods.* **10**, 508-513 (2013).

28. Susaki, E. A. et al. Versatile whole-organ/body staining and imaging based on electrolyte-gel properties of biological tissues. *Nature Communications.* **11**, 1982 (2020).

29. Kubota, S. I. et al. Whole-body profiling of cancer metastasis with single-cell resolution. *Cell Reports.* **20** (1), 236-250 (2017).

30. Gage, G. J., Kipke, D. R., Shain, W. Whole animal perfusion fixation for rodents. *Journal of Visualized Experiments.* **65**, e3564 (2012).

31. Bustamante, J. M. et al. A modified drug regimen clears active and dormant trypanosomes in mouse models of Chagas disease. *Science Translational Medicine.* **12** (567), eabb7656 (2020).

32. Wang, H., Khoradmehr, A., Tamadon, A. FACT or PACT: A comparison between free-acrylamide and acrylamide-based passive sodium dodecyl sulfate tissue clearing for whole tissue imaging. *Cell Journal.* **21** (2), 103-114 (2019).

33. Hofmann, J., Gadjalova, I., Mishra, R., Ruland, J., Keppler, S. J. Efficient tissue clearing and multi-organ volumetric imaging enable quantitative visualization of sparse immune cell populations during inflammation. *Frontiers in Immunology*. **11**, 599495 (2020).

34. Messal, H. A. et al. Antigen retrieval and clearing for whole-organ immunofluorescence by FLASH. *Nature Protocols.* **16**, 239-262 (2021).

35. Kolesova, H., Capek, M., Radochova, B., Janacek, J., Sedmera, D. Comparison of different tissue clearing methods and 3D imaging techniques for visualization of GFP-expressing mouse embryos and embryonic hearts. *Histochemistry and Cell Biology.* **146** (2), 141-152 (2016).

36. Chen, Y. et al. A versatile tiling light sheet microscope for imaging of cleared tissues. *Cell Reports.* **33**, 108349 (2020).